Vertical p-i-n germanium photodetector with high external responsivity integrated with large core Si waveguides

Ning-Ning Feng*[1], Po Dong[1], Dawei Zheng[1], Shirong Liao[1], Hong Liang[1], Roshanak Shafiiha[1], Dazeng Feng[1], Guoliang Li[2], John E. Cunningham[2], Ashok V. Krishnamoorthy[2], and Mehdi Asghari[1]

[1]*Kotura Inc., 2630 Corporate Place, Monterey Park, CA 91754, U.S.A.*
[2]*Sun Microsystems Inc., 9515 Towne Centre Dr., San Diego, CA 92121, U.S.A.*
**nfeng@kotura.com*

Abstract: We report a vertical p-i-n thin-film germanium photodetector integrated on 3μm thick large core silicon-on-insulator (SOI) waveguides. The device demonstrates very high external responsivity due to the low fiber coupling loss to the large core waveguides. The germanium width and thickness are carefully designed to achieve high responsivity yet retain high-speed performance. Even with fiber coupling loss included, the device has demonstrated greater than 0.7A/W external responsivity at 1550nm for TM polarization and 0.5A/W for TE polarization. A low dark current of 0.2μA at −0.5V bias is reported. 3dB bandwidths of 12GHz and 8.3GHz at −2.5V bias are also reported for 100μm and 200μm long devices, respectively. The device can cover the communication wavelength spectrum up to 1620nm with a relatively flat responsivity of >0.5A/W. Further studies suggest that with a modified design the device is capable of achieving 1A/W external responsivity for both TE and TM polarizations and greater than 30GHz bandwidth.

©2009 Optical Society of America

OCIS codes: (230.5160) Photodetectors; (130.3120) Integrated optics devices; (130.0250) Optoelectronics; (200.4650) Optical interconnects.

References and links

1. L. C. Kimerling, D. Ahn, A. B. Apsel, M. Beals, D. Carothers, Y.-K. Chen, T. Conway, D. M. Gill, M. Grove, C.-Y. Hong, M. Lipson, J. Liu, J. Michel, D. Pan, S. S. Patel, A. T. Pomerene, M. Rasras, D. K. Sparacin, K.-Y. Tu, A. E. White, and C. W. Wong, "Electronic-photonic integrated circuits on the CMOS platform," Proc. SPIE **6125**, 612502 (2006).
2. L. C. Kimerling, and L. Dal Negro, s. Saini, Y. Yi, D. Ahn, S. Akiyama, D. Cannon, J. Liu, J. G. sandland, D. Sparacin, J. Michel, K. Wada and M. R. Watts, "Monolithic silicon microphotonics," in Silicon Photonics: Topics in Applied Physics, L. Pavesi and D. J. Lockwood, eds., (Springer, Berlin, 2004) vol.94.
3. G. T. Reed, and A. Knights, Silicon Photonucs, (Wiley, 93–97, 2004).
4. L. Chen, and M. Lipson, "Ultra-low capacitance and high speed germanium photodetectors on silicon," Opt. Express **17**(10), 7901–7906 (2009).
5. L. Vivien, J. Osmond, J.-M. Fedeli, D. Marris-Morini, P. Crozat, J.-F. Damlencourt, E. Cassan, Y. Lecunff, and S. Laval, "42 GHz p.i.n Germanium photodetector integrated in a silicon-on-inculator waveguide," Opt. Express **16**, 6252 (2008).
6. J. Wang, W. Y. Loh, K. T. Chua, H. Zang, Y. Z. Xiong, S. M. F. Tan, M. B. Yu, S. J. Lee, G. Q. Lo, and D. L. Kwong, "Low-voltage high-speed (18GHz/1V) evanescent-coupled thin-file-Ge lateral PIN photodetectors integrated on Si waveguide," IEEE Photon. Technol. Lett. **20**(17), 1485–1487 (2008).
7. T. Yin, R. Cohen, M. M. Morse, G. Sarid, Y. Chetrit, D. Rubin, and M. J. Paniccia, "31 GHz Ge n-i-p waveguide photodetectors on Silicon-on-Insulator substrate," Opt. Express **15**(21), 13965–13971 (2007).
8. D. Ahn, C.-Y. Hong, J. Liu, W. Giziewicz, M. Beals, L. C. Kimerling, J. Michel, J. Chen, and F. X. Kärtner, "High performance, waveguide integrated Ge photodetectors," Opt. Express **15**(7), 3916–3921 (2007).
9. G. Dehlinger, S. J. Koester, J. D. Schaub, J. O. Chu, Q. C. Ouyang, and A. Grill, "High-speed Germanium-on-SOI lateral PIN photodiodes," IEEE Photon. Technol. Lett. **16**(11), 2547–2549 (2004).
10. S. Bidnyk, D. Feng, A. Balakrishnan, M. Pearson, M. Gao, H. Liang, W. Qian, C.-C. Kung, J. Fong, J. Yin, and M. Asghari, "Jeremy Yin, and M. Asghari, "Silicon-on-insulator-based planar circuit for passive optical network applications," IEEE Photon. Technol. Lett. **18**(22), 2392–2394 (2006).

#119896 - $15.00 USD Received 12 Nov 2009; revised 17 Dec 2009; accepted 17 Dec 2009; published 22 Dec 2009

11. N.-N. Feng, D. Feng, H. Liang, W. Qian, C.-C. Kung, J. Fong, and M. Asghari, “Low-loss polarization-insensitive Silicon-on-insulator-based WDM filter for triplexer applications,” IEEE Photon. Technol. Lett. **20**(23), 1968–1970 (2008).
12. Kotura Inc, *http://www.kotura.com/products/*.

1. Introduction

Silicon photonics has been an attractive research topic in recent years due to the potential capability of monolithic integration with complementary-metal-oxide-semiconductor (CMOS) microelectronic circuits [1–3]. It is widely recognized as the key technology to realize next generation interchip data communication through optical interconnects. Because of compatibility with CMOS technology, germanium (Ge)-based photodetectors have drawn much attention [4–9]. So far, all efforts at integrating Ge detectors on the silicon photonics platform have concentrated on small core submicron waveguides. Both evanescent [6–8] and butt [5] coupling schemes have been used to couple light from silicon waveguides to germanium layers. When integrated with small core waveguides, Ge photodetectors have the advantage of easier power transferring to the Ge films in the evanescent coupling case. However, small-waveguide-based Ge photodetectors suffer from larger fiber-coupling losses and tight fabrication tolerances, which make further integration of WDM components rather challenging, hence, preventing their widespread deployment in optical links and interconnects.

Large core silicon waveguides, on the other hand, are more tolerant to fabrication variations and have demonstrated superior performance in passive [10,11] and active devices [12]. Using linear-taper-based mode transformer technology, the fiber coupling loss to stand fiber can be as low as 0.5dB/facet for such devices [10–12]. This technology enables fabrication of waveguide-based Ge photodetectors that potentially achieve close to ideal performance. In this paper, we demonstrate a high-performance vertical p-i-n (VPin) Ge photodetector integrated on 3μm thick Silicon-on-insulator (SOI) waveguides. Due to the nature of large core, only evanescent or partial-butt coupling structures can be used to avoid large transient times associated to a thick Ge layer that would otherwise be necessary. This requires a phase matching condition to be satisfied between top Ge waveguide and bottom Si waveguide to efficiently transfer light from Si to Ge waveguides. In this design the phase match condition is achieved by carefully designing the Ge layer thickness and width. A flat spectrum of responsivity >0.5A/W all the way to the long-wavelength band (L-band) can be achieved with proper Ge thickness for TE polarization. For TM polarization, an external responsivity larger than 0.7A/W has been demonstrated. It is worthwhile pointing out that the responsivity reported here has taken the fiber-to-waveguide and waveguide propagation loss into accounted. The device also exhibits low dark current of 0.2μA (28mA/cm^2 current density) at −0.5V bias. 3dB bandwidths of 12GHz and 8.3GHz at −2.5V bias for 200μm and 200μm long devices are reported. Further studies suggest that with appropriate design modification a 1A/W external responsivity and larger than 30GHz bandwidth is achievable. The low driving voltage and low dark current make the device ready to be integrated with a trans-impedance amplifier (TIA) and used in optical data communication systems.

2. Device structure and fabrication

Schematic view of the reported large core waveguide-based vertical pin (VPin) Ge photodetector is shown in Fig. 1(a). The structure uses the evanescent coupling scheme. The fabrication process starts from 3μm thick SOI wafers with buried oxide. The single mode waveguide was formed by etching 1.2μm thick Si with a width of 3μm. The waveguide width in the Ge section is tapered up to accommodate different detector widths.

After silicon waveguide fabrication, the wafer was shallow-implanted with boron in the silicon waveguide surface and then heavily implanted in contact areas to form p-type ohmic contacts. The wafers went through a rapid-thermal-annealing (RTA) process at 1050°C for 5 second to activate the dopant. The Ge layer was selectively grown on top of the Si waveguide with a 100nm thick Ge buffer layer using low-temperature (400°C) growth followed by 1.1μm thick Ge growth at high-temperature (670°C). The film is intentionally grown thicker (1.1μm)

#119896 - $15.00 USD Received 12 Nov 2009; revised 17 Dec 2009; accepted 17 Dec 2009; published 22 Dec 2009
(C) 2010 OSA

than the target to compensate for the thickness reduction in later chemical-mechanical-polishing (CMP) steps. The wafers went through these CMP steps before post-growth-annealing. Figure 1(c) shows the cross-section TEM image of the structure after the CMP step. The measurement shows that the final thickness of the Ge film is 0.92μm.

The wafers then underwent a post-growth-annealing step to reduce the threading dislocations in the Ge film. The top of Ge film was implanted with phosphorus to form n-type ohmic contact area. After RTA activation, the metal contacts for both p and n were formed by depositing and patterning a Ti/Al metal stack on top of the doped areas. A top view SEM image of a typical fabricated device with length of 100μm is shown in Fig. 1(d). It is worthwhile to emphasize that the vertical pin junction in this design is formed only in the intrinsic Ge region and not in the intrinsic Si region. Therefore, the transient speed is solely determined by Ge thickness (not intrinsic Si thickness), thus enabling the realization of high speed large core detectors and their easy integration with large core silicon waveguides.

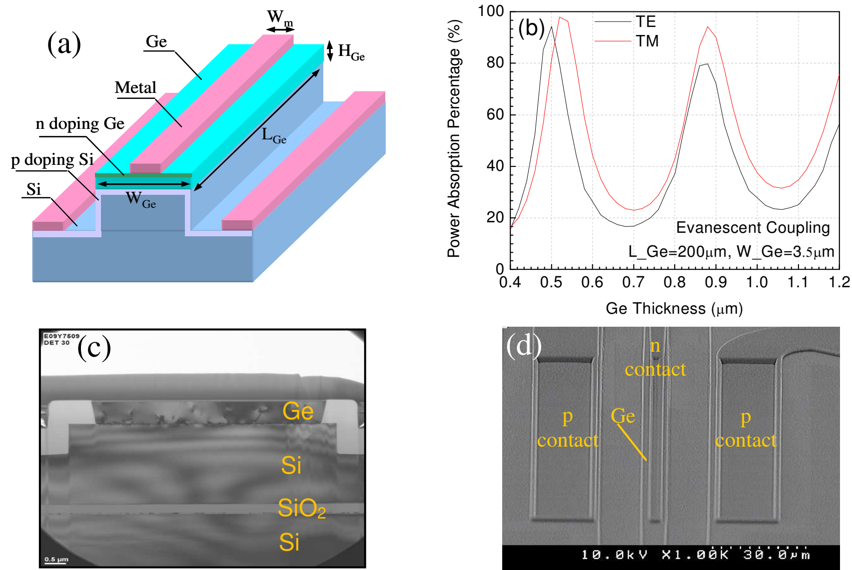

Fig. 1. (a) Schematic view of a vertical pin Ge waveguide photodetector integrated on top of a large core SOI waveguide. (b) Simulation results of power absorption by Ge versus Ge film thickness for the photodetector structure. (c) Cross-section TEM image of the fabricated device after CMT step (0.92μm Ge film on 3μm thick SOI waveguide). (d) Top view SEM image of the full-processed device.

The Ge thickness (H_{Ge}) is the key parameter to be optimized to realize maximum power absorption in the Ge layer. The beam propagation method (BPM, BeamProp, Rsoft Design Group) is used to provide a nominal design. Figure 1(b) shows the simulation results of the power absorption of a typical large-core-waveguide VPin Ge photodetector versus the Ge film thickness at a wavelength of 1550nm. The Ge width is 3.5μm and the length is 200μm. In our simulation, the metal absorption has been taken into account. The metal absorption turns out to be negligible. As indicated in this figure, the maximum absorption is realized at Ge thicknesses of around 0.5μm and 0.88μm, where the phase matching condition between the bottom SOI waveguide and the top Ge waveguide is satisfied for λ = 1550nm. As a leveraging parameter to tailor the responsivity spectrum, the Ge thickness can be made thicker to compensate for the Ge absorption coefficient dropping beyond 1570nm wavelength. This is used in the fabricated device reported here to enable an extended flat wavelength response. The final thickness of the fabricated device was measured to be 0.92um. As a result, the critical coupling point shifts to longer wavelength, therefore, the responsivity in L-band is considerably enhanced. As will be shown in the following section, the Ge thickness is indeed

#119896 - $15.00 USD Received 12 Nov 2009; revised 17 Dec 2009; accepted 17 Dec 2009; published 22 Dec 2009
(C) 2010 OSA

the key design parameter to manipulate the responsivity spectrum and extend the operating wavelength of the device into the long wavelength band (L-band).

3. Measurement results

The dark current I-V characteristics of a device with 200µm long and 3.5µm wide are shown in Fig. 2(a) and 2(b) for various temperatures. A low dark current of 0.2µA at −0.5V bias is achieved for this large area device. It corresponds to a current density of about 28mA/cm^2. Even at a temperature of 50°C, the device exhibits less than 1µA dark current as shown in Fig. 2(b). The low dark current is an evidence of a high-quality Ge film growth.

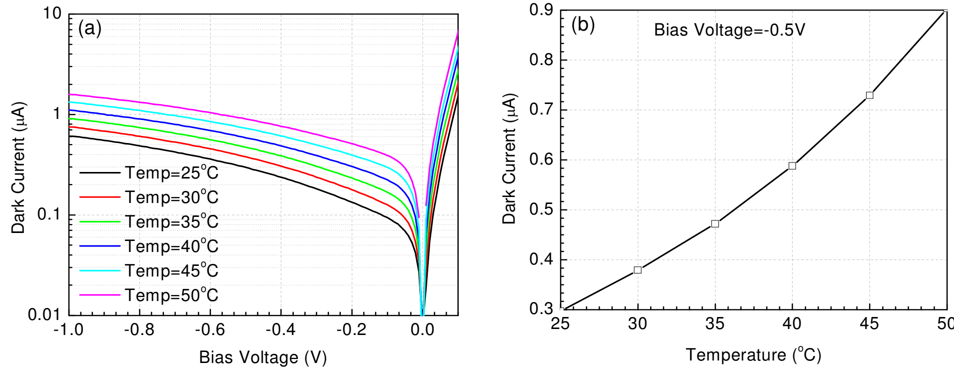

Fig. 2. (a) Dark current I-V characteristics for different temperatures of a Ge photodetector integrated on a large core SOI waveguide. (b) The temperature dependence of the device at bias voltage of −0.5V.

The photocurrent of the device under luminescence was measured using a lensed fiber pair with 3µm spot size. The waveguide propagation loss of this large core waveguide was measured with a spiral structure and is around 0.15dB/cm [8–10]. The lensed-fiber-to-waveguide coupling loss is measured to be about 1.2dB/facet using a reference passive waveguide. Coupling losses to standard fibers as small as 0.5dB/facet have been demonstrated using linear-taper based mode transformers [10–12] for this class of waveguides. The thicker Ge film leads to absorption reduction in short and central bands (S band and C band) due to red shifting of the critical coupling point. As a result, power leakage from the output side is expected for light with shorter wavelength. This power leakage can be measured as the excess loss of a SOI waveguide with Ge photodetector integrated on top compared to an identical reference passive waveguide without Ge film. The results are shown in Fig. 3(a). It shows that the phase matching points for both TE and TM polarization are shifted to longer wavelengths by using the thicker Ge film. The critical coupling points are measured at about 1605nm and 1585nm for TE and TM polarizations, respectively. It is noted that the excess loss of the active section is higher at critical coupling points. It is caused by the scattering loss at the output side Si/Ge interface, which does not contribute to the responsivity of the device.

When calculating the external responsivity (defined as the photocurrent/fiber input power), all power leaks from the photodetector are treated as part of the responsivity reduction and included in the calculation. In Fig. 3(b), the external responsivity of the reported device is shown for both TE and TM polarizations and marked with “External”. The TE responsivity is lower than that for TM due to the deliberate red-shifting of the critical coupling point resulting from the thicker Ge layer used. The TE coupling is more affected by the Ge thickness increase for the particular geometry and design of the waveguide used in this case. A flat responsivity spectrum of 0.5A/W is obtained up to 1580nm. A maximum responsivity of 0.72A/W is measured at 1600nm for the TE polarization. By intentionally decreasing the coupling in shorter wavelength and enhancing in longer wavelength, we are able to make the responsivity spectrum flat as shown in Fig. 3(b). For longer wavelength, the responsivity begins to decrease due to the dominant effect of the absorption decrease of Ge material as we discussed. For TM polarization, the responsivity remains at 0.8A/W up to 1580nm wavelength. All

#119896 - $15.00 USD Received 12 Nov 2009; revised 17 Dec 2009; accepted 17 Dec 2009; published 22 Dec 2009
(C) 2010 OSA

results are measured at a bias of −0.5V. Due to the low propagation losses in these larger core waveguides, Fabry-Perot (FP) oscillations are observed in these measurements.

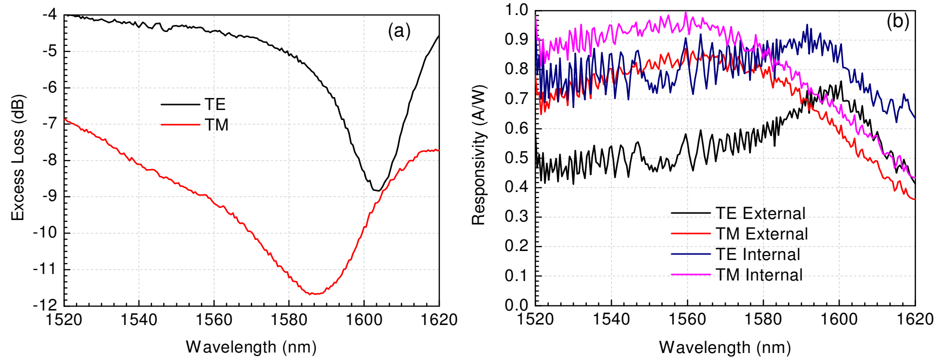

Fig. 3. (a) Excess loss of a SOI waveguide with Ge film on top compared to a reference passive waveguide without Germanium. (b) The measured external and calculated internal responsivities of the device.

It is interesting to note that the results shown in Fig. 3(b) also suggest that, if the output power is excluded from the responsivity evaluation the internal responsivity for both TE and TM can be very high if the Ge thickness is chosen to ensure phase matching at shorter wavelengths. For TM polarization, the internal responsivity can reach 1A/W. In other words, with longer device with right Ge thickness, we are able to achieve close to ideal performance. Moreover, even with fiber coupling loss included (0.5dB/facet), the responsivities can be as large as 0.7A/W and 0.9A/W for TE and TM polarizations, respectively.

The frequency response of the device was measured using an Agilent vector network analyzer (AVN). The high-speed RF signal from AVN was applied to an external modulator with a bandwidth of ~40GHz. The output modulated light signal was input into the detector and the photocurrent was then measured by a high-speed RF probe. The system was calibrated in advance to factor out the effect of the RF systems, including the cable, the bias-tee, and the modulator. The frequency responses of a 200μm long Ge photodetector are shown in Fig. 4(a) for different bias voltages. The device demonstrates an 8.3GHz 3dB bandwidth with −2.5V bias voltage. Further investigation reveals that the device speed is limited by the RC time constant. The series resistance and capacitance of this device are measured to be 33Ω and 200fF. Taking the 50 Ω cable impedance into account, it sets the RC constant limited speed to be 9.5GHz, which is coincident with our measurement result. The bias voltage dependence of the 3dB bandwidth shown in the insert of Fig. 4(a) may indicate that the device speed is limited by the RC constant since higher bias reduces the device capacitance.

In Fig. 4(b), the measured 3dB bandiwidth results of devices with different Ge widths are shown. With −2.5V bias, a 100μm long device can reach 12GHz speed. However, such device demonstrates a smaller responsivity of around 0.4A/W. Initial analysis indicates that the transient-time-limited speed of the device can be as fast as 30GHz given the thickness of the Ge film. However, in our case, the devices are RC-constant limited. Through processing optimization, the series resistance and capacitance can be reduced; the devices can operate at 30GHz speed.

#119896 - $15.00 USD Received 12 Nov 2009; revised 17 Dec 2009; accepted 17 Dec 2009; published 22 Dec 2009
(C) 2010 OSA

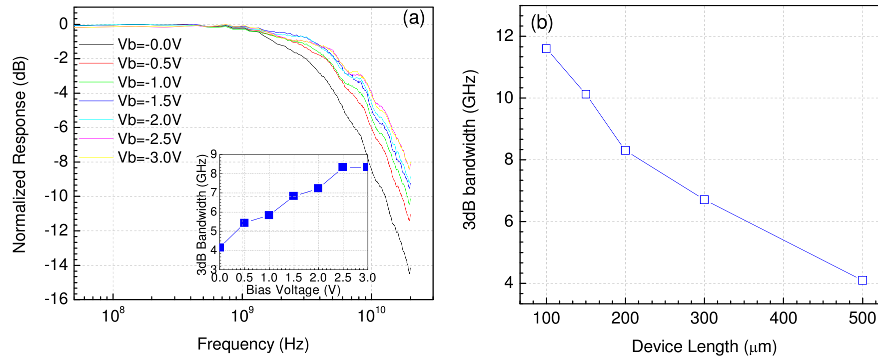

Fig. 4. (a) Frequency response of a 200μm device with different bias voltage. (b) 3dB bandwidth f_{3dB} versus the device length.

A solution enabling both higher speed and higher responsivity can be based on the use of a partially butt-coupled structure. Instead of growing Ge layer on top of Si waveguide, a small Ge growing window (trench) can be opened by partially etching the Si waveguide and the required Ge thickness (for example 0.92μm) selectively grown into the opened trench. Due to the higher coupling strength resulting from this structure, a shorter device length is possible. Simulations show that this modified device can achieve both high responsivity and high speed. The 3dB bandwidth of such devices is expected to be greater than 30GHz with the resopnsivity approaching 1A/W.

4. Conclusions

We report a high-speed vertical p-i-n thin-film Ge photodetector integrated on 3μm thick large core SOI waveguides. The devices demonstrate larger than 0.7A/W external responsivity including fiber-to-waveguide losses. A low dark current of around 0.2μA is also reported for a 200X3.5μm large-area device. The reported devices have achieved 12GHz and 8.3GHz 3dB bandwidths for 100μm and 1200μm long devices, respectively. In addition, it is demonstrated that the responsivity spectrum can be tailored by choosing different Ge thickness designs. The reported device covers the entire S-, C-, and L-bands of the optical communication window. Further study shows that device performance can be significantly improved by using butt coupling schemes. The 3dB bandwidth of such devices are predicted to be larger than 30GHz. Integrated on large core SOI waveguide, the device shows very good robustness to tolerances in its fabrication process and has great potential for application in next generation data communication systems and inter-chip optical interconnects.

Acknowledgement

The authors acknowledge funding of this work by DARPA MTO office under UNIC program supervised by Jagdeep Shah (contract agreement with SUN Microsystems HR0011-08-9-0001). The authors greatly acknowledge Dr. C. C. Kung, Dr. Joan Fong, and Dr. Wei Qian from Kotura Inc. for their work in fabricating of the device, and Dr. Xuezhe Zheng from SUN Microsystems for helpful discussions. The views, opinions, and/or findings contained in this article/presentation are those of the author/presenter and should not be interpreted as representing the official views or policies, either expressed or implied, of the Defense Advanced Research Projects Agency or the Department of Defense. The paper is approved for public release and distribution unlimited.

#119896 - $15.00 USD Received 12 Nov 2009; revised 17 Dec 2009; accepted 17 Dec 2009; published 22 Dec 2009
(C) 2010 OSA